DALTON
FULL PAPER

$[Ni(L)(MeCN)][BF_4]_2$ {L = 2,5,8-trithia[9],(2,9)-1,10-phenanthrolinophane} as a building block for the synthesis of binuclear nickel(II) complexes: X-ray crystal structure and magnetochemistry of a singly F-bridged nickel(II) dimer

Alexander J. Blake,[a] Francesco A. Devillanova,[b] Alessandra Garau,[b] Andrew Harrison,[c] Francesco Isaia,[b] Vito Lippolis,*[b] Satish K. Tiwary,[c] Martin Schröder,[a] Gaetano Verani[b] and Gavin Whittaker[c]

[a] *School of Chemistry, The University of Nottingham, Nottingham, UK NG7 2RD*
[b] *Dipartimento di Chimica Inorganica ed Analitica, Università degli Studi di Cagliari, SS 554 Bivio per Sestu, 09042 Monserrato (CA), Italy*
[c] *Department of Chemistry, The University of Edinburgh, West Mains Road, Edinburgh, UK EH9 3JJ*

Received 13th August 2002, Accepted 24th September 2002
First published as an Advance Article on the web 29th October 2002

The substitution reactions of the coordinated acetonitrile molecule in $[Ni(L)(MeCN)][BF_4]_2$ (**1**) {L = 2,5,8-trithia-[9],(2,9)-1,10-phenanthrolinophane} with three potentially bidentate ligands L′ (L′ = N_3^-, 4,4′-bipyridine and F^-) have been studied both in solution and in the solid state with the aim of verifying the potential of **1** as a starting material for the synthesis of $[\{Ni(L)\}_2L']^{n+}$ (n = 3, 4) Ni^{II}-binuclear compounds. While the mononuclear $[Ni(L)(N_3)]BF_4$ complex was isolated in the solid state from the reaction of **1** with N_3^-, the binuclear $[\{Ni(L)\}_2F][BF_4]_3 \cdot MeCN \cdot H_2O$ and $[\{Ni(L)\}_2(4,4'\text{-bipy})][BF_4]_4$ compounds have been obtained from the reactions of **1** with F^- and 4,4′-bipy, respectively. The first two complexes have been characterised by X-ray diffraction studies. In $[Ni(L)(N_3)]^+$, a distorted octahedral geometry is achieved at the Ni^{II}, with five sites occupied by the macrocyclic ligand L and the sixth by a monodentate azide group. In $[\{Ni(L)\}_2F]^{3+}$, two $[Ni(L)]^{2+}$ units are bridged by a fluoride ligand to give only the second example of a singly F-bridged Ni^{II} dimer. The magnetisation of $[\{Ni(L)\}_2F][BF_4]_3 \cdot MeCN \cdot H_2O$ and of $[\{Ni(L)\}_2(4,4'\text{-bipy})][BF_4]_4$ has been recorded over the temperature range 1.8–300 K and indicates a significant antiferromagnetic exchange in the former.

Introduction

Hetero- and homo-binuclear complexes of Ni^{II} have attracted much attention over recent years because of their interesting structural and magnetic properties, and because of their ability to model the active sites of metalloproteins such as urease and Ni-containing hydrogenase.[1] The nature of the bridging groups is of paramount importance in determining the metal–metal distance and, consequently, in mediating the magnetic coupling interactions between the two paramagnetic metal centres.[2] Many examples of Ni^{II}-binuclear complexes containing single bridging groups, such hydroxo,[3] oxalato,[4] nitrito,[5] cyanato,[6] thiocyanato[7] and, in particular, azido ligands,[8] and complexes containing double[8j,9] and triple bridges[8h–j,10] have been reported. In particular, the Ni^{II}–(azido)$_n$–Ni^{II} (n = 1, 2, 3) system is the most extensively studied because of the distinctive magneto-structural relationship between the coordination mode adopted by the azido bridge and the resulting magnetic behaviour of the Ni^{II}-binuclear framework: end-to-end coordination (Ni^{II}–N–N–N–Ni^{II}) is associated with antiferromagnetic exchange,[8–10] whereas end-on coordination, with the two metal centres joined by the same N-donor of the azide group, is characterised by ferromagnetic exchange.[8–10]

Interestingly, while polynuclear Ni^{II}-compounds featuring double and triple halide bridges are quite common in the literature,[11–16] to the best of our knowledge (including a recent search of the Cambridge Crystallographic Database),[17] only five examples of Ni^{II}-binuclear complexes having a single μ-halide bridge have been structurally characterised, and these are: $[(bzmi)_4ClNi(\mu\text{-}Cl)NiCl(bzmi)_4]^+$,[18] $[(pyN_4)Ni(\mu\text{-}Cl)Ni(pyN_4)]^{3+}$[19] and $[\{\eta^2,\eta^4\text{-}(Et_8N_4Ni)\}_2Ni_2(\mu\text{-}Cl)]^-$[20] {bzmi = benzimidazole, pyN_4 = 2,6-bis(1′,3′-diamino-2′-methylprop-2′-yl)pyridine, Et_8N_4 = 5,5,10,10,15,15,20,20-octaethylporphyrinogen}, all containing a single chloride bridge, $[(bipy)_2FNi(\mu\text{-}F)NiF(bipy)_2]^+$ {bipy = 2,2′-bipyridine},[21] which has a single fluoride bridge, and $[\{Ni([16]aneN_5)\}_2(\mu\text{-}Br)]^{3+}$ {[16]aneN$_5$ = 1,4,7,10,13-pentaazacycloexadecane},[22] which has a single bromide bridge.

Recently, we reported the synthesis of new mixed aza-thioether crowns incorporating the 1,10-phenanthroline sub-unit and their coordinating properties towards d^8 transition metal ions.[23] In particular, in the case of Ni^{II},[23a] the complex $[Ni(L)(MeCN)][BF_4]_2$ (**1**) {L = 2,5,8-trithia[9],(2,9)-1,10-phenanthrolinophane} has been synthesised and structurally characterised: L acts as an N_2S_3 pentadentate donor encapsulating the metal centre within a cavity having a square-based pyramidal stereochemistry, with an MeCN molecule completing an overall octahedral coordination sphere around the metal centre.

The coordinated MeCN molecule can be readily substituted by anionic or neutral ligands,[24] offering a useful route to other pseudo-octahedral Ni^{II} complexes. Since L can block five sites of an octahedral coordination sphere, it could, in principle, allow the synthesis of Ni^{II}-binuclear complexes having a single bridging exogenous ligand. In order to verify the potential of $[Ni(L)(MeCN)][BF_4]_2$ (**1**) as a precursor for the synthesis of Ni^{II}-binuclear compounds having the $[Ni(L)]^{2+}$ cation as building block, we have considered the reactions of **1** with NaN_3, 4,4′-bipyridine and $Bu_4NF \cdot H_2O$.

This journal is © The Royal Society of Chemistry 2002

Results and discussion

Reaction of **1** with 0.5 molar equivalents of sodium azide in MeCN gave a pink solution from which red–brown crystals were obtained by slow diffusion of Et_2O. Similar crystals were obtained using a 1 : 1 reaction molar ratio. The fast-atom bombardment (FAB) mass spectrum of the product exhibits peaks with the correct isotopic distribution for $[^{58}Ni(L)(N_3)]^+$ ($m/z = 458$) and for $[^{58}Ni(L)]^+$ ($m/z = 416$), and the IR spectrum shows a sharp and very intense band at 2040 cm^{-1}, typical of the antisymmetric stretching vibration of a coordinated azide ligand. A single crystal structure determination was undertaken to ascertain the nuclearity of the complex, and confirms the product to be the mononuclear cation $[Ni(L)(N_3)]^+$ (Fig. 1, Table 1). The geometry about the metal centre is pseudo-octahedral, with five coordination sites occupied by the chelating ligand L and a monodentate azide group completing the coordination sphere. The bond distances and angles between the Ni^{II} ion and the donor atoms of L are similar to those observed for other octahedral Ni^{II} complexes obtained from **1** *via* replacement of the MeCN molecule by different anions.[23a,24] The Ni–N(3) distance involving the azide group [2.037(4) Å] is shorter than typical values for azide-bridged Ni^{II}-binuclear systems, which range from 2.110 to 2.170 Å,[8–10] but similar to those found in octahedral Ni^{II} complexes bearing a terminal coordinated N_3^- ligand (2.05–2.12 Å).[25–28] The Ni–N(3)–N(4) angle of 122.4(3)° is in the normal range (120–142°) observed for Ni^{II} complexes featuring either terminal or bridging azide ligands.[8g,j,9a,10,25–28]

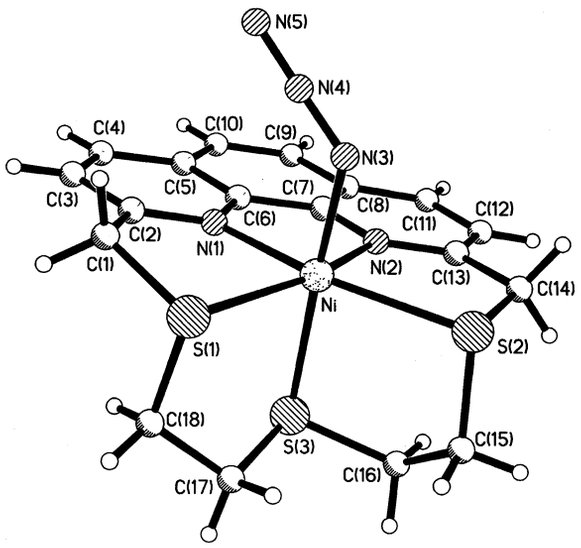

Fig. 1 View of the cation $[Ni(L)(N_3)]^+$ with the numbering scheme adopted. Heavy atoms are not shown as ellipsoids and the BF_4^- anion is omitted for clarity.

In an attempt to synthesise Ni^{II}-binuclear complexes by substitution of the MeCN molecule in $[Ni(L)(MeCN)][BF_4]_2$ (**1**) with neutral bidentate ligands, we reacted **1** with 0.5 equivalents of 4,4′-bipyridine (4,4′-bipy) in MeCN, a microcrystalline product was isolated after crystallisation by Et_2O vapour diffusion. Elemental analysis suggested the formulation $[\{Ni(L)\}_2(4,4'\text{-bipy})][BF_4]_4$ for this product, which is also obtained when using a 1 : 1 reagent molar ratio, but, unfortunately, no single crystals suitable for X-ray diffraction studies were obtained. In previous papers, we have reported the synthesis of the mononuclear complexes $[Ni(L)I]I_3$,[23a] $[Ni(L)Cl]BF_4\cdot dmf$[23a] and $[Ni(L)Br]BF_4$,[24] obtained by reacting **1** with the appropriate halide ion in a 1 : 1 molar ratio in MeCN, and for the first two complexes structural analyses were also possible. We therefore reacted **1** with $Bu_4NF\cdot H_2O$ under the same experimental conditions (1 : 1 molar ratio in MeCN) and purple crystals were grown from the reaction mixture *via* Et_2O vapour diffusion. Although the FAB mass spectrum did not show any evidence for an Ni^{II}-binuclear species, elemental analysis and IR spectroscopic data did suggest the formation of the binuclear complex cation $[\{Ni(L)\}_2F]^{3+}$. In fact, the infrared spectrum of the crystalline product in the low frequency region shows two peaks at 377 and 363 cm^{-1}, typical of the stretching vibration modes of an asymmetric Ni–F–Ni′ system.[12,13,21] A crystal structure determination showed the stoichiometry to be $[\{Ni(L)\}_2F][BF_4]_3\cdot MeCN\cdot H_2O$ and confirmed the formation of a singly F-bridged Ni^{II} dimer (Fig. 2, Table 1). The bridge is essentially symmetric, with Ni–F distances of 1.967(3) and 1.973(2) Å, and an Ni–F–Ni′ angle of 161.31(12)°. The distance between the two Ni^{II} ions is 3.887(1) Å and the phenanthroline moieties in the two $[Ni(L)]^{2+}$ units face each other and lie on almost parallel planes at a mean distance of about 3.70 Å. However, the $[Ni(L)]^{2+}$ units are rotated with respect to each other along

Table 1 Selected bond lengths (Å) and angles (°) for $[Ni(L)(N_3)]BF_4$ and $[\{Ni(L)\}_2F][BF_4]_3\cdot MeCN\cdot H_2O$ with standard deviations in parentheses[a]

	$[Ni(L)(N_3)]BF_4$	$[\{Ni(L)\}_2F][BF_4]_3\cdot MeCN\cdot H_2O$[b]
Ni–N(1)	2.025(3)	2.013(3) [2.034(4)]
Ni–N(2)	2.036(3)	2.031(4) [2.037(3)]
Ni–S(1)	2.4662(12)	2.4278(15) [2.4306(14)]
Ni–S(2)	2.4557(13)	2.4527(15) [2.4735(15)]
Ni–S(3)	2.4158(12)	2.3892(14) [2.4091(14)]
Ni–X	2.037(4)	1.967(3) [1.973(2)]
N(1)–Ni–N(2)	80.71(13)	81.11(14) [80.89(14)]
N(1)–Ni–S(1)	81.12(10)	81.81(11) [81.52(10)]
N(1)–Ni–S(2)	162.41(10)	161.52(11) [161.77(10)]
N(1)–Ni–S(3)	92.34(10)	89.71(11) [93.79(11)]
N(1)–Ni–X	93.09(16)	93.56(12) [93.64(13)]
N(2)–Ni–S(1)	160.73(10)	162.84(9) [162.39(11)]
N(2)–Ni–S(2)	81.71(10)	81.10(9) [80.97(11)]
N(2)–Ni–S(3)	88.99(10)	93.56(11) [94.78(10)]
N(2)–Ni–X	96.54(16)	89.99(13) [94.72(12)]
S(1)–Ni–S(2)	116.27(5)	116.06(5) [116.63(5)]
S(1)–Ni–S(3)	85.40(4)	87.96(5) [87.27(5)]
S(1)–Ni–X	90.79(13)	89.46(9) [85.49(8)]
S(2)–Ni–S(3)	86.76(5)	86.46(5) [85.85(5)]
S(2)–Ni–X	89.48(13)	91.38(8) [89.71(9)]
S(3)–Ni–X	172.81(14)	175.51(7) [168.75(7)]
Ni–X–Ni′		161.31(12)

[a] X = N(3) (N_3^-) and F for complexes $[Ni(L)(N_3)]BF_4$ and $[\{Ni(L)\}_2F][BF_4]_3\cdot MeCN\cdot H_2O$, respectively. [b] Values in square brackets refer to the bond distances and angles involving the Ni′ centre (see Fig. 2).

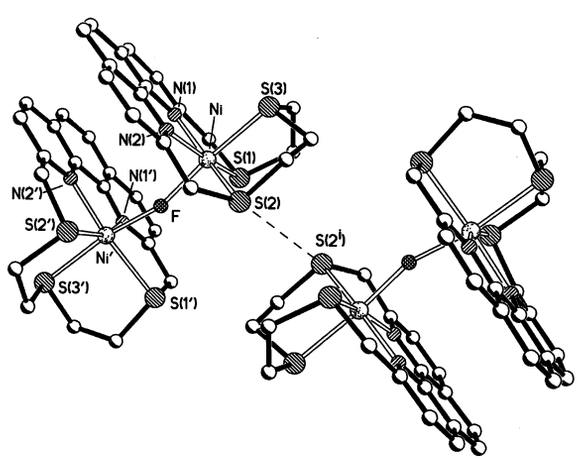

Fig. 2 View of the cation $[\{Ni(L)\}_2F]^{3+}$ with the numbering scheme adopted. Heavy atoms are not shown as ellipsoids and hydrogen atoms and counter anions are omitted for clarity. Symmetry code: (i) $-x$, $-y$, $-z$.

the Ni–Ni′ axis, as indicated by the N(2)–Ni–Ni′–N(2′) torsion angle of 56.05(13)°, and the projection of one phenanthroline moiety does not superimpose on the top of the other. Pairs of $[\{Ni(L)\}_2F]^{3+}$ cations related by inversion interact with each other *via* S ··· S contacts of 3.546(3) Å (Fig. 2). As already mentioned, structurally characterised complexes containing a single Ni^{II}–X–Ni^{II} halide bridge are rare and, to the best of our knowledge, $[\{Ni(L)\}_2F]^{3+}$ is only the second reported example of an Ni^{II}-binuclear system featuring a single Ni^{II}–F–Ni^{II} bridge. In $[(bipy)_2FNi(\mu\text{-}F)NiF(bipy)_2]^{+}$,[21] the Ni–F bond distance [1.985(3) Å] is slightly longer than those observed in $[\{Ni(L)\}_2F]^{3+}$ and the Ni–F–Ni angle [170.8(2)°] is much closer to linearity, with an Ni–Ni distance of 3.956 Å. The weak π–π interaction between the phenanthroline moieties in $[\{Ni(L)\}_2F]^{3+}$ (the two phenanthroline moieties lie on almost parallel planes at a mean distance of about 3.70 Å) may be responsible for these differences and might also explain why only mononuclear Ni^{II} complexes have been isolated from the reaction of **1** with the bigger Cl^-, Br^- and I^- halogenide anions. Indeed, an almost linear μ-Cl, μ-Br or μ-I bridge between two $[Ni(L)]^{2+}$ units would set the two phenanthroline moieties too far away from each other, thus hampering any π–π interaction between the two aromatic systems.

We have previously studied the substitution of the coordinated MeCN molecule in **1** by UV-visible spectrophotometric titrations.[24] We found that while substitution with anionic ligands such as Cl^-, Br^-, I^- and SCN^- is quantitative, reaction with neutral ligands, L′, is governed by the equilibrium

$$[Ni(L)(MeCN)]^{2+} + L' \rightleftharpoons [Ni(L)(L')]^{2+} + MeCN \quad (1)$$

Quantitative substitution of the MeCN molecule has also been observed with the N_3^- ligand; the initial electronic spectrum of **1** changes isosbestically upon adding increasing amounts of NaN_3 until a 1 : 1 $[N_3^-]$/[**1**] molar ratio is reached [Fig. 3(a)]. The plot of absorbance values at 970 nm *vs.* the $[N_3^-]$/[**1**] molar ratio shows two straight lines intersecting at an $[N_3^-]$/[**1**] value of 1.

With 4,4′-bipy, a change in the UV-visible spectrum is observed during the spectrophotometric titration, even beyond the 1 : 1 [4,4′-bipy]/[**1**] molar ratio [Fig. 3(b)], indicating an equilibrium reaction. The presence of at least one isosbestic point [Fig. 3(b)] indicates that only two absorbing species are involved in the substitution reaction, in agreement with eqn. 1 above, a fact that has also been confirmed by factor analysis[29] of the electronic spectra recorded after each addition of 4,4′-bipy. Using a non-linear least-squares program,[24,30] the formation constant for the 1 : 1 $[Ni(L)(4,4'\text{-bipy})]^{2+}$ complex was calculated as 270.7(3). Therefore, it appears that upon addition of 4,4′-bipy to **1**, only the 1:1 $[Ni(L)(4,4'\text{-bipy})]^{2+}$ species is formed in solution over the whole range of reaction molar ratios, despite the fact that the relatively insoluble binuclear $[\{Ni(L)\}_2(4,4'\text{-bipy})]^{4+}$ complex is the only species isolated in the solid state using either a 0.5 : 1 or 1 : 1 [4,4′-bipy] : [**1**] molar ratio.

In the spectrophotometric titration of **1** with $Bu_4NF{\cdot}H_2O$, the isosbestic point is maintained up to a $[F^-]$/[**1**] molar ratio of 0.5 (Fig. 4), indicating the formation of a binuclear Ni^{II} species. Beyond this $[F^-]$/[**1**] value, the spectral changes suggest the transformation of the initially formed complex toward other species. Significantly, over the whole range of $[F^-]$/[**1**] molar ratios explored, the binuclear complex $[\{Ni(L)\}_2F]^{3+}$ is the only compound isolated as a solid.

The magnetisation of polycrystalline samples of $[\{Ni(L)\}_2F][BF_4]_3{\cdot}MeCN{\cdot}H_2O$ and $[\{Ni(L)\}_2(4,4'\text{-bipy})][BF_4]_4$ was measured over the temperature range 1.8–300 K, then converted to susceptibility and corrected for the diamagnetic contributions of the sample holder and the constituent atoms of the samples.[31]. Fig. 5 shows plots against temperature of the susceptibility, χ_m, and effective magnetic moment, μ_{eff}, per mol

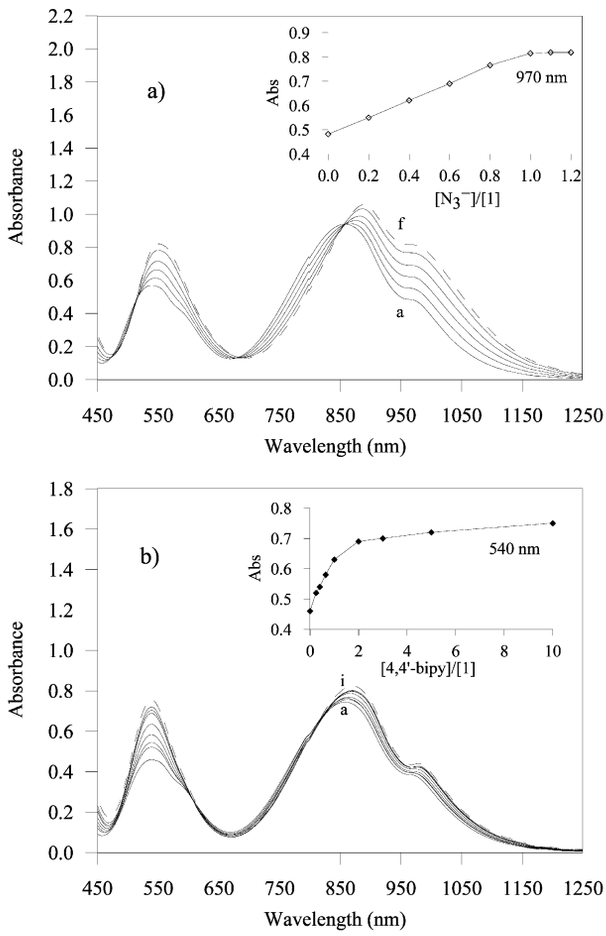

Fig. 3 UV-visible spectra of MeCN solutions of $[Ni(L)(MeCN)][BF_4]_2$ (**1**) and (a) NaN_3, [**1**] = 1.6×10^{-2} mol dm^{-3} and $[NaN_3]$ = 0, 3.12×10^{-3}, 6.23×10^{-3}, 9.35×10^{-3}, 1.25×10^{-2} and 1.56×10^{-2} mol dm^{-3} for spectra a–f, respectively; and (b) 4,4′-bipy, [**1**] = 1.19×10^{-2} mol dm^{-3} and [4,4′-bipy] = 0, 3.03×10^{-3}, 4.85×10^{-3}, 7.58×10^{-3}, 1.21×10^{-2}, 2.42×10^{-2}, 3.64×10^{-2}, 6.0×10^{-2} and 0.12 mol dm^{-3} for spectra a–i, respectively. For clarity, only the first and the last of these spectra have been labelled. The dashed lines indicate spectra recorded for 1 : 1 [L′]/[**1**] molar ratios (L′ = N_3^- and 4,4′-bipy) and correspond, respectively, to the spectra of pure $[Ni(L)(N_3)]^+$ and $[\{Ni(L)\}_2(4,4'\text{-bipy})]^{4+}$ at the same concentrations in dmf. The insets show plots of the absorbance values *vs.* the [L′]/[**1**] molar ratio at 970 and 540 nm for L′ = N_3^- and 4,4′-bipy, respectively.

of Ni in $[\{Ni(L)\}_2F][BF_4]_3{\cdot}MeCN{\cdot}H_2O$, as calculated from the relation $\mu_{eff} = 2.828(\chi_m T)^{1/2}$. For a paramagnetic system of spin-only moments corresponding to $S = 1$, the effective moment is expected to be $\sim\sqrt{8} \cong 2.828$ BM, while the value we observed at 300 K was 2.47 BM, dropping significantly as the temperature was lowered (Fig. 5). This indicates significant antiferromagnetic exchange in this material. Closer inspection of the data also reveals a discontinuity in the region 200–220 K. In the absence of structural data above this point, we can only speculate on the possible reasons for this feature: a change in structure could lead to a change in the ligand field experienced by the magnetic centres, with a concomitant change in effective moment per ion, alternatively, structural changes could alter the strength of exchange. Resolution of this uncertainty requires crystal structure data taken above this apparent transition. Even at 210 K the structure exhibits disorder of the BF_4^- anions. Given that such disorder becomes harder to model at elevated temperatures, leading to a reduction in the precision of the overall structure, we felt there would be no advantage in determining the crystal structure at a higher temperature. Unfortunately, the anomaly in the region 200–220 K cannot be studied, even by NMR spectroscopy, because of the very low solubility of the complex in all common solvents. This

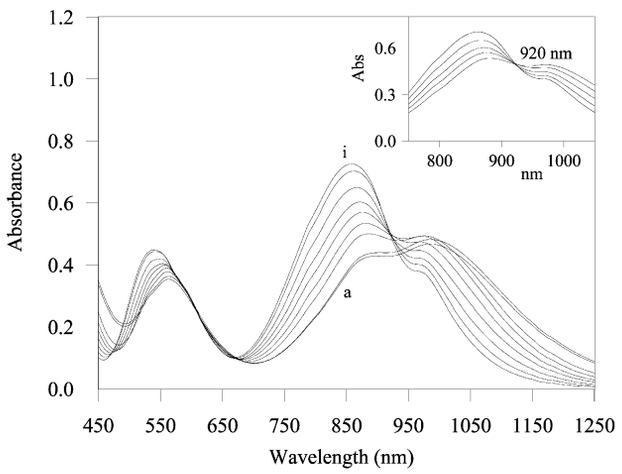

Fig. 4 UV-visible spectra of MeCN solutions of $[Ni(L)(MeCN)][BF_4]_2$ (**1**) and $Bu_4NF{\cdot}H_2O$, [**1**] = 1.12×10^{-2} mol dm^{-3} and $[Bu_4NF{\cdot}H_2O]$ = 0, 2.23×10^{-3}, 3.72×10^{-3}, 5.21×10^{-3}, 7.44×10^{-3}, 8.93×10^{-3}, 1.04×10^{-2}, 1.19×10^{-2} and 1.49×10^{-2} mol dm^{-3} for spectra a–i, respectively. For clarity, only the first and the last of these spectra have been labelled. The inset shows the isosbestic point at 920 nm observed during the titration up to $[F^-]/[\mathbf{1}] = 0.5$.

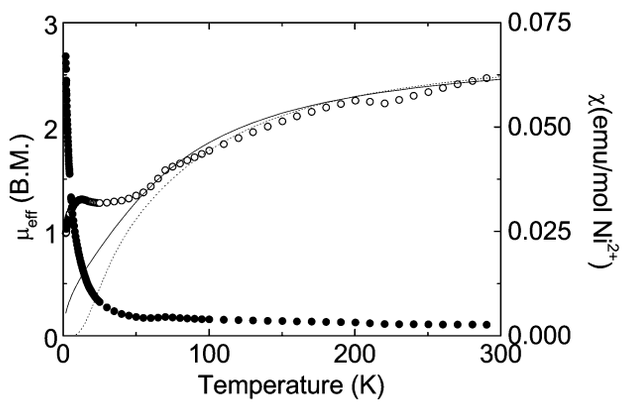

Fig. 5 Temperature dependence of the effective magnetic moment, μ_{eff} (○), and magnetic susceptibility per mole of Ni^{II}, χ (●), for $[\{Ni(L)\}_2F][BF_4]_3{\cdot}MeCN{\cdot}H_2O$. The solid and dashed lines represent the best manual fits of the expressions for the effective moments of an S = 1 linear antiferromagnetic chain and an antiferromagnetically coupled dimer, respectively.

discontinuity restricts analysis of the high temperature susceptibility data, constraining fits to a Curie–Weiss expression to temperatures in the region 240–300 K. When we attempted to perform a fit to the Curie–Weiss expression for S = 1, we obtained a non-physical value for g (3.16 ± 0.32), and an unusually high value for the Curie temperature θ (660 ± 86 K). This suggests that even in this temperature range, short range magnetic correlations invalidate the mean-field approximation.

The structure of the compound indicates that, in addition to the μ-F bridge between the Ni centres, there is the possibility of exchange through S ··· S contacts. The distance between these centres [3.546(3) Å] is significantly less than twice the van der Waals radius of S (typically 1.85 Å) and it is known that magnetic exchange may be significant between such atoms with this separation or greater.[32] We anticipate that our susceptibility data could be fitted either to some form of dimer model, or to an alternating antiferromagnetic Heisenberg chain model, with stronger and weaker exchange, J and αJ, respectively (where the alternation parameter, α, lies within the limits $0 \leq \alpha \leq 1$). In the latter case, the spin Hamiltonian, $\boldsymbol{H}$, for such a system[33] may be written as $\boldsymbol{H} = -J\Sigma\boldsymbol{S}_{2i}\boldsymbol{S}_{2i+1} + \alpha J\Sigma\boldsymbol{S}_{2i}\boldsymbol{S}_{2i-1}$. As no analytical treatment yet exists for an S = 1 system, two limiting cases were considered.

Case 1: $\alpha = 0$. In this case, the Hamiltonian becomes that of isolated dimers, for which an analytical expression is available[33] and is given as $\mu_{eff}^2 = 3g^2[\exp(x) + 5\exp(3x)]/[1 + 3\exp(x) + 5\exp(3x)]$, where $x = J/k_BT$). The experimental data were manually fitted to the above expression over the full temperature range, giving optimised values of the fit parameter χ^2 for g = 2.0 and $J = -40$ cm^{-1}. This fit is shown in Fig. 5 as a dashed line.

Case 2: $\alpha = 1$. This case corresponds to a linear Heisenberg chain model with S = 1. Although there is no analytical solution of this model, there is a parametrised form of the Bonner–Fisher curves,[33] which gives the effective moment as $\mu_{eff}^2 = g^2N/D$, where $N = 2 + 0.0194x + 0.777x^2$ and $D = 3 + 4.346x + 3.232x^2 + 5.834x^3$. A manual best fit to the experimental data over the full temperature range gave g = 2 and $J = -67$ cm^{-1}. This fit is shown as a solid line in Fig. 5.

It should be noted that the quality of these fits is not perfect. In addition to the discontinuity around 200–220 K, there is also clearly more complex behaviour in the lowest temperature data. The poor fit in the low temperature region is not surprising, as the compound is expected to behave as an alternating antiferromagnet ($0 < \alpha < 1$) and not as one of the limiting cases. Further neighbour exchange or, more probably, ligand-field effects (which, in this context, may also be referred to as 'zero-field splitting')[31] may also produce deviations from our simple model. In any event, we find that the exchange between Ni centres through the fluoride bridge is significant and antiferromagnetic. The only comparable Ni^{II} dimer containing an Ni–X–Ni bridge where X is a halogen is $[(pyN_4)Ni(\mu\text{-}Cl)Ni(pyN_4)][PF_6]_3$ {pyN_4 = 2,6-bis(1′,3′-diamino-2′-methylprop-2′-yl)pyridine},[19] where susceptibility data were treated very successfully with a simple dimer model with an exchange constant of $J = -74$ cm^{-1}. The Ni–X–Ni bridging angle in that case is 165.5(3)° for X = Cl, while for X = F in $[\{Ni(L)\}_2F][BF_4]_3{\cdot}MeCN{\cdot}H_2O$, the corresponding angle is 161.31(12)°. In general, magnetic exchange through this type of bridge is expected to decrease as the angle subtended at the halogen is reduced from 180°. We would also anticipate that exchange is stronger for an Ni–X–Ni bridge as X is changed from F to Cl, as observed in the well-characterised family of extended solids of general formula A_2NiX_4 (where A is typically K, Rb or Cs, and X is typically F, Cl or Br), which adopt the K_2NiF_4 structure.[34]

The magnetic behaviour of the $[\{Ni(L)\}_2(4,4'\text{-bipy})][BF_4]_4$ compound was much more straightforward, and the temperature dependence of both the susceptibility and the effective moment are plotted in Fig. 6. The susceptibility data fitted well to a Curie-Weiss expression and, with S = 1, the least-squares fit yielded g = 2.135(7) and $\theta = -1.44(1)$ K; a TIP contribution of $170 \times 1\ 0^{-6}$ emu mol^{-1} was also extracted from the fit.

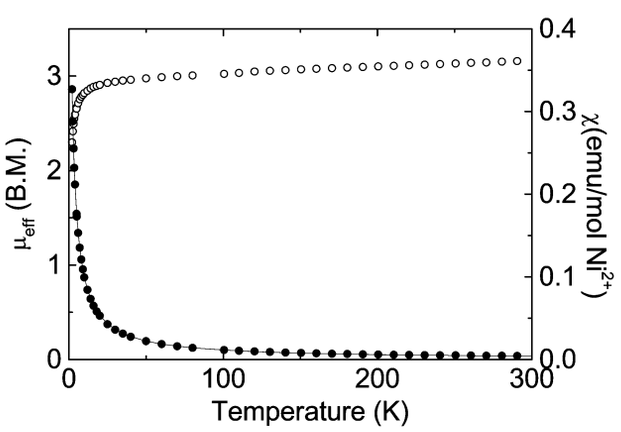

Fig. 6 Temperature dependence of the effective magnetic moment, μ_{eff} (○), and magnetic susceptibility per mole of Ni^{II}, χ (●), for $[\{Ni(L)\}_2(4,4'\text{-bipy})][BF_4]_4$. The solid line is a least-squares fit of a Curie–Weiss expression to the susceptibility data.

Experimental

General

All melting points are uncorrected. Microanalytical data were obtained by using a Fisons EA 1108 CHNS-O instrument operating at 1000 °C. FAB mass spectra (3-nitrobenzyl alcohol matrix) were recorded at the School of Chemistry, University of Nottingham, UK. Infrared spectra were recorded on a Bruker IFS55 spectrometer at room temperature from either polythene pellets using a Mylar beam splitter and polythene windows (500–50 cm^{-1}) or KBr pellets using a KBr beam splitter and KBr windows (4000–400 cm^{-1}). UV-visible measurements were carried out in MeCN solution using a Varian Cary 5 UV-visible-NIR spectrophotometer equipped with a temperature controller accessory and connected to an IBM PS/2 computer. The spectra recorded during titrations with N_3^- and 4,4′-bipy were analysed using the program SPECFIT[29] in order to determine the number of species present in solution. In the case of the reaction with 4,4′-bipy, the same spectra were also employed to calculate the value of K_{eq} using a program based on a non-linear least-squares method.[30] This program assumes that the best values of K_{eq} and ε are those which minimise the sum of the function $\chi^2 = \Sigma(A_c - A_s)^2/(N - 2)$, where A_c and A_s are the calculated and the experimental absorbances, and N is the number of data points. The optimisation of K_{eq} was carried out using four different wavelengths.

The magnetisation of $[\{Ni(L)\}_2F][BF_4]_3\cdot MeCN\cdot H_2O$ and $[\{Ni(L)\}_2(4,4'\text{-bipy})][BF_4]_4$ was recorded over the temperature range 1.8–300 K using a Quantum Design $MPMS_2$ SQUID magnetometer in applied fields of 100 or 1000 G, then converted to susceptibility and corrected for the diamagnetic contributions of the gelatine sample holder and the constituent atoms of the sample using Pascal′s constants.[31]

Complex **1** was synthesised according to the procedure previously reported.[23] The UV-visible spectra of several solutions were recorded in the range 450–1250 nm at 25 °C, keeping the concentration of **1** constant and varying that of L′ (N_3^-, F^-, 4,4′-bipy) up to a [L′]/[**1**] molar ratio of 1.2 for N_3^- and F^- (beyond this limit, a solid starts precipitating) and *ca.* 10 for 4,4′-bipy. All the compounds and solvents used in the synthesis of the complexes were obtained from Aldrich Chemical Company and used without further purification.

Syntheses

$[Ni(L)(N_3)]BF_4$. Addition of NaN_3 (2.5 mg, 0.04 mmol) to a solution of **1** (50 mg, 0.079 mmol) in MeCN, followed by crystallisation from MeCN–Et_2O afforded red–brown crystals of $[Ni(L)(N_3)]BF_4$ (20 mg, 48% yield), m.p. 220 °C with decomposition [Found (calc.) for $C_{18}H_{18}BF_4N_5NiS_3$ (%): C, 39.9 (39.6); H, 3.6 (3.3); N, 13.0 (12.8); S, 17.5 (17.6)]. FAB MS: *m*/*z* 458, 416; calc. for $[^{58}Ni(L)(N_3)]^+$ and $[^{58}Ni(L)]^+$ 459 and 417, respectively. UV-visible (dmf), λ/nm (ε_{max}/dm^3 mol^{-1} cm^{-1}): 551 (156), 910 (77), 1019 (53). IR, ν/cm^{-1}: 3425s, 3080w, 3000w, 2920w, 2040s, 1660w, 1590m, 1575m, 1485m, 1420m, 1410m, 1400m, 1370m, 1280w, 1150m, 1090s, 1050m, 940w, 900m, 860m, 830w, 730w, 690w, 630m, 530w, 350w.

$[\{Ni(L)\}_2(4,4'\text{-bipy})][BF_4]_4$. Addition of 4,4′-bipyridine (6 mg, 0.038 mmol) to a solution of **1** (50 mg, 0.079 mmol) in MeCN, followed by crystallisation from MeCN/Et_2O, afforded pink solid $[\{Ni(L)\}_2(4,4'\text{-bipy})][BF_4]_4$ (50 mg, 50% yield), m.p. 270 °C with decomposition [Found (calc.) for $C_{46}H_{44}B_4F_{16}N_6Ni_2S_6$ (%): C, 41.6 (41.3); H, 3.7 (3.3); N, 6.6 (6.3); S, 14.4 (14.4)]. FAB MS: *m*/*z* 416; calc. for $[^{58}Ni(L)]^{2+}$ 417. UV-visible (dmf), λ/nm (ε_{max}/dm^3 mol^{-1} cm^{-1}): 544 (81), 891 (105) and 976 (81). IR, ν/cm^{-1}: 3420s, 2980w, 2925m, 1610s, 1590s, 1535w, 1490s, 1420s, 1375w, 1290m, 1230m, 1050s, 940m, 890m, 850m, 820m, 730m, 690m, 640m, 520m.

$[\{Ni(L)\}_2F][BF_4]_3\cdot MeCN\cdot H_2O$. Addition of $Bu_4NF\cdot H_2O$ (10.3 mg, 0.039 mmol) to a solution of **1** (50 mg, 0.079 mmol) in MeCN, followed by crystallisation from MeCN/Et_2O, afforded purple crystals of $[\{Ni(L)\}_2F][BF_4]_3\cdot MeCN\cdot H_2O$ (50 mg, 57% yield), m.p. 260 °C with decomposition [Found (calc.) for $C_{38}H_{41}B_3F_{13}N_5Ni_2OS_6$ (%): C, 38.9 (38.8); H, 3.3 (3.2); N, 5.3 (5.1); S, 17.6 (17.3)]. FAB MS: *m*/*z* 416; calc. for $[^{58}Ni(L)]^{2+}$ 417. UV-visible (dmf), λ/nm (ε_{max}/dm^3 mol^{-1} cm^{-1}): 550 (108), 893 (83) and 979 nm (78 dm^3 mol^{-1} cm^{-1}). IR, ν/cm^{-1}: 3627s, 3197s, 3072s, 2963m, 1650w, 1620w, 1593s, 1576s, 1500m, 1486m, 1430m, 1422m, 1398m, 1285w, 1046s, 935w, 884m, 858m, 804w, 724w, 693w, 654w, 535m, 377m, 363m.

Table 2 Summary of crystal data for $[Ni(L)(N_3)]BF_4$ and $[\{Ni(L)\}_2F][BF_4]_3\cdot MeCN\cdot H_2O$

Compound	$[Ni(L)(N_3)]BF_4$	$[\{Ni(L)\}_2F][BF_4]_3\cdot MeCN\cdot H_2O$
Formula	$C_{18}H_{18}BF_4N_5NiS_3$	$C_{38}H_{41}B_3F_{13}N_5Ni_2OS_6$
M_w	546.08	1172.96
Crystal system	Triclinic	Triclinic
Space group	$P\bar{1}$	$P\bar{1}$
a/Å	7.2069(6)	12.471(5)
b/Å	11.0525(8)	12.777(3)
c/Å	14.0537(8)	15.590(2)
α/°	104.688(7)	96.16(2)
β/°	95.563(9)	97.46(2)
γ/°	100.377(11)	107.63(2)
U/Å^3	1053.11(13)	2319.0(11)
D_c/g cm^{-3}	1.722	1.680
Z	2	2
T/K	298(2)	210(2)
μ(Mo-Kα)/mm^{-1}	1.271	1.174
Reflections collected	4234	6430
Unique reflections, R_{int}	3718, 0.0589	6061, 0.0698
Observed reflections $[I > 2\sigma(I)]$	3016	4261
T_{min}, T_{max}	0.672, 0.827	0.696, 0.816
R_1	0.0463	0.0688
wR_2 (all data)	0.1170	0.1794

Crystal structure determinations

Details of the data collection and refinement of the structures are reported in Table 2. Only special features of the analysis are noted here. The crystal of $[\{Ni(L)\}_2F][BF_4]_3\cdot MeCN\cdot H_2O$ was cooled using an Oxford Cryosystem open-flow nitrogen cryostat.[35] For both structures, data were collected on a Stoë Stadi-4 four-circle diffractometer using ω–θ scans. Data were corrected for Lorentz and polarisation effects and absorption corrections were applied using ψ-scans. Both structures were solved by direct methods using SHELXS-97[36] and full-matrix least-squares refinement on F^2 was performed using SHELXL-97.[37] All non-H atoms were refined anisotropically and H atoms were introduced at calculated positions and thereafter incorporated into a riding model with $U_{iso}(H) = 1.2U_{eq}(C)$. Two of the three BF_4^- anions in $[\{Ni(L)\}_2F][BF_4]_3\cdot MeCN\cdot H_2O$ exhibited disorder of their F atoms, which were each modelled over two equally occupied sites. Appropriate restraints to the B–F distances and F–B–F angles were also applied during refinement.

CCDC reference numbers 191665 and 191666.

See http://www.rsc.org/suppdata/dt/b2/b207934h/ for crystallographic data in CIF or other electronic format.

Acknowledgements

We thank the Ministero dell'Istruzione dell'Università e della Ricerca (M.I.U.R.) and the Engineering and Physical Science Research Council (EPSRC) for support.

References

1 (*a*) R. Cammack, *Adv. Inorg. Chem.*, 1988, **32**, 297; (*b*) V. McKee, *Adv. Inorg. Chem.*, 1993, **40**, 323; (*c*) A. C. Marr, D. J. E. Spencer and M. Schröder, *Coord. Chem. Rev.*, 2001, **219**, 1055.

2 (*a*) *Magneto-Structural Correlations in Exchange Coupled Systems*, ed. R. Willet, D. Gatteschi and O. Khan, NATO ASI Ser., Ser. C, Reidel, Dordrecht, 1985, p. 40; (*b*) C. J. Cairns and D. H. Busch, *Coord. Chem. Rev.*, 1986, **69**, 1; (*c*) P. McCarthy and H. Güdel, *Coord. Chem. Rev.*, 1988, **88**, 69; (*d*) S. M. Gorun and S. Lippard, *Inorg. Chem.*, 1991, **30**, 1625.
3 (*a*) P. Chaudhuri, H.-J. Kuppers, K. Wieghardt, S. Gehring, W. Haase, B. Nuber and J. Weiss, *J. Chem. Soc., Dalton Trans.*, 1988, 1367; (*b*) L. Ballester, E. Coronado, A. Gutiérrez, A. Monge, M. F. Perpiñán, E. Pinilla and T. Rico, *Inorg. Chem.*, 1992, **31**, 2053.
4 P. Roman, C. Guzman-Miralles, A. Luque, J. I. Beitia, J. Cano, F. Lloret, M. Julve and S. Alvarez, *Inorg. Chem.*, 1996, **35**, 3741.
5 (*a*) A. Meyer, A. Gleizes, J. J. Girerd, M. Verdaguer and O. Kahn, *Inorg. Chem.*, 1982, **21**, 1729 and references therein; (*b*) A. Escuer, R. Vicente and X. Solans, *J. Chem. Soc., Dalton Trans.*, 1997, 531.
6 A. Escuer, R. Vicente, M. S. El Fallah, X. Solans and M. Font-Bardia, *J. Chem. Soc., Dalton Trans.*, 1996, 1013 and references therein.
7 M. Monfort, J. Ribas and X. Solans, *Inorg. Chem.*, 1994, **33**, 4271 and references therein.
8 (*a*) R. Vicente, A. Escuer, J. Ribas and X. Solans, *Inorg. Chem.*, 1992, **31**, 1726; (*b*) A. Escuer, R. Vicente, J. Ribas, M. S. El Fallah and X. Solans, *Inorg. Chem.*, 1993, **32**, 1033; (*c*) A. Escuer, R. Vicente, J. Ribas, M. S. El Fallah, X. Solans and M. Font-Bardia, *Inorg. Chem.*, 1993, **32**, 3727; (*d*) A. Escuer, R. Vicente, J. Ribas, M. S. El Fallah, X. Solans and M. Font-Bardia, *J. Chem. Soc., Dalton Trans.*, 1993, 2975; (*e*) A. Escuer, R. Vicente, J. Ribas, M. S. El Fallah, X. Solans and M. Font-Bardia, *Inorg. Chem.*, 1994, **33**, 1842; (*f*) G. A. McLachlan, G. D. Fallon, R. L. Martin, B. Moubaraki, K. S. Murray and L. Spiccia, *Inorg. Chem.*, 1994, **33**, 4663; (*g*) R. Vicente, A. Escuer, J. Ribas, M. S. El Fallah, X. Solans and M. Font-Bardia, *Inorg. Chem.*, 1995, **34**, 1278; (*h*) J. Ribas, M. Monfort, B. K. Ghosh, R. Cortes, X. Solans and M. Font-Bardia, *Inorg. Chem.*, 1996, **35**, 864; (*i*) A. Escuer, R. Vicente, M. S. El Fallah, S. B. Kumar, F. A. Mautner and D. Gatteschi, *J. Chem. Soc., Dalton Trans.*, 1998, 3905; (*j*) J. Ribas, A. Escuer, R. Vicente, M. Font-Bardia, R. Cortes, L. Lezoma and T. Rojio, *Coord. Chem. Rev.*, 1999, **193–195**, 1027.
9 (*a*) C. G. Pierpont, D. N. Hendrickson, D. M. Duggan, F. Wagner and E. K. Barefield, *Inorg. Chem.*, 1975, **14**, 604; (*b*) J. Ribas, M. Monfort, C. Diaz, C. Bastos and X. Solans, *Inorg. Chem.*, 1993, **32**, 3557.
10 (*a*) P. Chaudhuri, M. Guttmann, D. Ventur, K. Wieghardt, B. Nuber and J. Weiss, *J. Chem. Soc., Chem. Commun.*, 1985, 1618; (*b*) P. Chaudhuri, T. Wayhermuller, E. Bile and K. Wieghardt, *Inorg. Chim. Acta*, 1996, **252**, 195.
11 S. J. Higgins and W. Levason, *Inorg. Chim. Acta*, 1986, **113**, 47.
12 F. J. Rietmeijer, J. G. Haasnoot, A. J. Den Hartog and J. Reedijk, *Inorg. Chim. Acta*, 1986, **113**, 147.
13 J. Reedijk and R. W. M. ten Hoedt, *Recl. Trav. Chim. Pays-Bas*, 1982, **101**, 49.
14 M. M. Brezinski, J. Schneider, L. J. Radonovich and K. J. Klabunde, *Inorg. Chem.*, 1989, **28**, 2414.
15 J. Verbiest, J. A. C. van Ooijen and J. Reedijk, *J. Inorg. Nucl. Chem.*, 1980, **42**, 971.
16 R. W. M. ten Hoedt and J. Reedijk, *Inorg. Chim. Acta*, 1981, **51**, 23.
17 (*a*) F. H. Allen and O. Kennard, *Chem. Des. Autom. News*, 1993, **8**(1), 1; (*b*) F. H. Allen and O. Kennard, *Chem. Des. Autom. News*, 1993, **8**(1), 31–37; . Cambridge Structural Database version 5.23, released April 2002.
18 M. G. B. Drew, D. H. Templeton and A. Zalkin, *Inorg. Chem.*, 1968, **7**, 2618.
19 C. Dietz, F. W. Heinemann, J. Kuhnigk, C. Kruger, M. Gerdan, A. X. Trautwein and A. Grohmann, *Eur. J. Inorg. Chem.*, 1998, 1041.
20 L. Bonomo, E. Solari, M. Latronico, R. Scopelliti and C. Floriani, *Chem. Eur. J.*, 1999, **5**, 2040.
21 J. Emsley, M. Arif, P. A. Bates and M. B. Hursthouse, *J. Chem. Soc., Dalton Trans.*, 1989, 1273.
22 J. C. A. Boeyens and E.-L. Oosthuizen, *J. Crystallogr. Spectrosc. Res.*, 1992, **22**, 3.
23 (*a*) A. J. Blake, F. Demartin, F. A. Devillanova, A. Garau, F. Isaia, V. Lippolis, M. Schröder and G. Verani, *J. Chem. Soc., Dalton Trans.*, 1996, 3705; (*b*) F. Contu, F. Demartin, F. A. Devillanova, A. Garau, F. Isaia, V. Lippolis, A. Salis and G. Verani, *J. Chem. Soc., Dalton Trans.*, 1997, 4401.
24 A. J. Blake, J. Casabò, F. A. Devillanova, L. Escriche, A. Garau, F. Isaia, V. Lippolis, R. Kivekas, V. Muns, M. Schröder, R. Sillanpää and G. Verani, *J. Chem. Soc., Dalton Trans.*, 1999, 1085.
25 J. Ribas, M. Monfort, B. Kumar Ghosh, X. Solans and M. Font-Bardia, *Polyhedron*, 1996, **15**, 1091.
26 M. K. Urtiaga, M. I. Arriortua, I. G. De Muro and R. Cortes, *Acta Crystallogr., Sect. C*, 1995, **51**, 62.
27 P. Jian, S. Wang, J. Suo, L. Wang and Q. Wu, *Acta Crystallogr., Sect. C*, 1995, **51**, 1071.
28 F. Paap, W. L. Driessen, J. Reedijk, B. Kojic-Prodic and A. L. Spek, *Inorg. Chim. Acta*, 1985, **104**, 55.
29 H. Gampp, M. Maeder, C. J. Meyer and A. Zuberbühler, *Talanta*, 1985, **32**, 95.
30 G. Crisponi and V. Nurchi, *J. Chem. Educ.*, 1989, **66**, 54.
31 R. L. Carlin, *Magnetochemistry*, Springer, Berlin, 1986.
32 A. S. Batsanov, A. J. Moore, N. Robertson, A. Green, M. R. Bryce, J. A. K. Howard and A. E. Underhill, *J. Mater. Chem.*, 1997, **7**, 387.
33 O. Kahn, *Molecular Magnetism*, VCH Publishers, New York, 1993.
34 L. J. de Jongh and A. R. Miedema, *Adv. Phys.*, 1974, **23**, 1.
35 J. Cosier and A. M. Glazer, *J. Appl. Crystallogr.*, 1986, **19**, 105.
36 G. M. Sheldrick, *Acta Crystallogr., Sect. A*, 1990, **46**, 467.
37 G. M. Sheldrick, SHELXL-97, Universität Göttingen, Germany, 1997.